[1.]Saliu Ojo SEIDU, [2.]Sheriff Olalekan SAKA,
[3.]Bolarinwa Johnson KUTELU, [4.]Hakeem OWOKUNLE

CHILLING TENDENCY OF IRON POWDER TREATED GREY CAST IRON

[1,2,4.] Department of Metallurgical and Materials Engineering, Federal University of Technology, Akure, NIGERIA
[3.]Department of Minerals and Petroleum Resources Engineering, Federal Polytechnic Ado-Ekiti, NIGERIA

Abstract: This study investigated the chilling tendency of iron powder treated grey cast iron. Chill wedges of type W_1, W_2 and W_3, specified in the ASTM A 367 with respective cooling moduli- CM of 0.11 cm, 0.23 cm and 0.35 cm) were poured in sand mould at varied (0.2wt% and 0.4wt%) iron powder addition with constant (0.3wt%) Ca, Zr, Al- FeSi alloy using ladle inoculation. The treated and double treated irons solidified within the strongly hypereutectic range (CE= 4.60-4.89). The chill evaluation parameters were measured and evaluated. The 0.2wt% Fe powder +0.3wt% FeSi alloy was observed to have given the optimum iron powder addition with best intermediate chilling result for W_1 and W_2 while the single treated iron (0.3wt% FeSi alloy) at all wedge samples gave best inoculating effect in sequential order of W_3, W_2 and W_1. The microstructure reveals uniformly distributed and randomly oriented moderate graphite flakes particularly at slower rate of cooling and undercooled graphite (Types B and D) at high cooling rate as these corroborate with the chilling evaluations.
Keywords: chilling, iron powder, chill wedges, graphite morphology, grey cast iron

1. INTRODUCTION

Basically, cast irons are iron carbon alloys containing carbon more than 2%, i.e., more than maximum solid solubility of carbon in austenite. However, cast irons are eutectic ferrous iron carbon alloys, which means that the eutectic reaction occurs during solidification [1] of the various types of cast iron, grey iron still remain the common commercial and most extensively used iron in industry especially automobile application due to its specific and unique properties such as; most economical choice, good castability, low melting point (1148-1250°C), very good machinability, good resistance to wear, high damping capacity, high compressive strength, high thermal conductivity, good resistance to atmospheric corrosion, notch insensitive, etc [1]. However, in some cases, the engineering applications of grey cast iron which make it the most widely used variety are based on weight [2].

Grey cast iron solidification is such that when it is fulfilled, three possible structures do phase out - the grey, mottle and white structures. As a result, the slow rates of solidification and cooling are more likely to influence the formation of grey iron structures likewise a small value of undercooling or small chilling could also favours the grey iron structure formation [3]. Meanwhile, chilling tendency is the transition of liquid iron from graphite to cementite in cast iron [4]. Cast iron with high chilling tendency will definitely develop either white or mottled iron structure thereby possessing high brittleness and in turn poor machinability [5].

Among other factors that are particularly relevant to chilling behaviour during solidification (primary and eutectic solidification) are the relative nucleation and growth rate of graphite and cementite [1,6]. The primary solidification of grey iron starts with the formation of primary austenite dendrites. While the austenite dendrites form, more carbon diffuse into the remaining liquid iron until the carbon composition becomes eutectic, the second stage of solidification (eutectic solidification) begins. However, it is during this stage that the growth of graphite, eutectic austenite and eutectic cells are formed in the microstructure. Researches on grey cast iron production and properties are increasing due to some defects still experience during casting. Among those defects are gas porosity, shrinkage porosity, and penetration problems which deteriorate the quality, and influence the grey cast iron production [7]. In another work, this type of defect was studied and characterized. It was found that this type of defect seems to be located around the primary austenite crystals, or dendrites, suggesting that the primary solidification and how its solidification structure is developed become important [8]. Besides, primary austenite dendrites are also essential for the strength [9, 10].

Iron powder has been used as inoculants for the primary solidification and considered to be the most effective nucleating particle for primary austenite dendrites due to the fact that its crystallographic structure is the same as the primary phase of the solidifying metal and also owing to the fact that the pure iron powder does not melt [11]. Knowing that the eutectic solidification depends on the primary solidification, as iron powder was added to the melt, while the eutectic cell size could be related to the secondary dendrite arm spacing (SDAS). Secondary dendrite arm spacing, on the other hand, is related to the solidification time [12].

Therefore, the need to control the chilling tendency by inoculation (FeSi alloy) and promote primary solidification by iron powder addition can be achieved. This study therefore investigated the effect of iron powder additions with conventional inoculants on strongly hypereutectic grey cast irons which will invariably have a significant effect on the structural properties of the grey cast iron that will meet the desired results for automobile industries. However, in this work, wedge sample is applied similar to the conventional method of testing the tendency of molten iron to solidify grey, mottle and white.

2. MATERIALS AND METHOD

- Materials
The materials used for this work are scrap auto engine block, ferrosilicon (FeSi) based alloy (CAS Pty Ltd), Iron Powder (Fe - powder), graphite and Limestone.

- Production of Grey Cast Iron
The charge was heated in a 40kg graphite crucible furnace. The scraps of 20kg were first charged through the opening of the crucible and subsequently 15kg was charged during melting, 0.5kg of furnace inoculants (FeSi alloy) and graphite were added respectively. The crucible furnace was superheated to 1,520°C, and at this temperature, the charges had become melt completely and ready for tapping. Iron powder and FeSi alloy inoculant (74.22% Si, 1.21% Al, 1.21% Zr, 2.44% Ca) of particle sizes in the range 0.3 to 0.7 mm were added to the metal stream when tapping from the crucible to preheated ladle at 1,490°C temperature. The first melt was treated with 0.3wt% FeSi alloy only (single treated) while the subsequent melts were double treated with respective varying iron powder at 0.2 and 0.4 wt% plus constant amount of 0.3 wt% FeSi inoculant. Standard chill wedges of W_1, W_2, and W_3, specified in the ASTM A367-wedge test were explored [13] for the experiment. The cooling moduli CM of the test samples are 0.21cm, 0.35cm and 0.47m for W_1, W_2 and W_3 respectively. After pouring the melt into the prepared green sand moulds, the castings were left for almost twenty-four hours. The fettled cast chill wedge samples were fracture at the centre (midway of its length) in order to carry out macrostructure (fracture) analysis for the different treatments. The measurements of chills were obtained for each treatment by evaluating the following chill parameters: relative clear chill (RCC); relative mottled chill (RMC) and relative total chill (RTC) as shown in equations 1 – 3 [13]:

$$RCC = 100(W_C/B) \tag{1}$$
$$RTC = 100(W_C/B) \tag{2}$$
$$RMC = 100(W_m/B) = 100[0.5(W_t + W_c)/B] \tag{3}$$

Where, W_c is the clear chill zone of the wedge (portion nearest the apex, entirely free of any grey spots); W_m is the mottled zone (portion starting with the end of the clear chill and continuing to the last spot of visible cementite or white iron); W_t is the total chill zone (from the junction of the grey fracture with the first appearance of chilled iron to the apex); and B is the maximum width of the test wedge. Hence, the figure below indicates the three different zones- grey, mottled and white iron zones marked as point 1, 2, 3.

- Characterization
The metallography examinations were done on each point of the wedge sample. The samples were examined under a metallurgical microscope at a magnification of 200 and the micrographs of the un-etched samples were obtained following standard procedure. The chemical composition of each wedge samples was analyzed for each of the iron treatments.

Figure 1: Points 1, 2 and 3 indicate White, Mottle and Grey Iron Zones Representing W_t, W_m and W_c Respectively.

3. RESULTS AND DISCUSSION

- Chemical composition
The chemical analysis of the experimental produced irons in Table 1 showed the carbon content in the range (3.61-4.04); silicon content, Si (2.45-2.91); manganese content, Mn (0.35-0.59); sulphur, S (0.14-0.164); and phosphorus, P (0.06-0.11). Typical residual elements were negligible because of their low levels. However, from the analysis, the evaluation of carbon equivalent CE proved that the produced cast irons fall within the hypereutectic cast irons.

- Macrostructure analysis
Tables 2, 3, and 4 show the results of the chill criteria obtained and evaluated from the fractured irons produced (wedge samples). Figures 2, 3, and 4 show the results obtained from the macrostructure of the

fractured wedge samples for irons produced. For all irons produced, the double treated irons (0.4wt% Fe-powder+0.3wt% FeSi) was recorded to have high chilling tendency from W_1 through W_2 up to W_3 for all chill criteria in particular RCC. However, the single treated iron (0.3wt% FeSi) was observed to have shown minimum chill tendency despite the small addition rate and poor ladle treatment compared with the large addition rate [14] and with the typical values [12-15]. Hence, the single treated iron shows a consistent trend in reducing the chill for all wedge samples from RCC through RMC up to RTC. This indicates the efficiency of the inoculant, chemical composition and likewise the effect of the casting thickness or cooling modulus. Generally, the chilling tendency decreases with increasing cooling modulus or casting thickness that is from W_1 up to W_3 wedge samples for all iron treatments with minimal variation at the chilling criteria evaluated. This was as a result of cooling rate, that is W_1- CM= 0.11cm at a fast rate of cooling than W_2 (CM= 0.21cm) and W_3- CM= 0.35cm (medium cooling rate) or as the cooling modulus values increases the chill tendency decreases [17].

Table 1: Chemical analysis of produced irons

Irons	Chemical Composition (wt %)						C.E	Mn/S	Mn x S
	C	Si	Mn	P	S	Al			
0.3wt% FeSi	3.61	2.91	0.59	0.067	0.146	0.0073	4.60	4.04	0.086
0.2wt%Fe-powder+0.3wt% FeSi	3.99	2.49	0.359	0.111	0.164	0.0013	4.86	2.19	0.059
0.4wt%Fe-powder+0.3wt% FeSi	4.04	2.45	0.354	0.106	0.140	‹0.001	4.89	2.53	0.050

Table 2: Macrostructure Analysis of W_1

Iron Treatment	W_1: Chill Parameters					
	W_c (mm)	W_m (mm)	W_t (mm)	RCC %	RMC %	RTC %
0.3wt% FeSi alloy	1.18	2.40	3.61	12.97	26.72	39.67
0.2wt% Fe powder +0.3wt% FeSi alloy	2.72	3.55	4.38	29.89	39.01	48.13
0.4wt% Fe powder +0.3wt% FeSi alloy	2.94	4.03	5.11	32.31	44.23	56.15

Wedge = W1; Width B=9.1mm; CM=0.11cm

Table 3: Macrostructure Analysis of W_2

Iron Treatment	W_2: Chill Parameters					
	W_c (mm)	W_m (mm)	W_t (mm)	RCC%	RMC %	RTC %
0.3wt% FeSi alloy	1.71	3.23	4.74	12.30	23.20	34.10
0.2wt% Fe powder +0.3wt% FeSi alloy	2.36	3.62	4.88	16.98	26.05	35.11
0.4wt% Fe powder +0.3wt% FeSi alloy	2.42	4.21	6.00	17.41	30.29	43.17

Wedge = W2; Width B=13.9mm; CM=0.21cm

Table 4: Macrostructure Analysis of W3

Iron Treatment	W3: Chill Parameters					
	Wc (mm)	Wm (mm)	Wt (mm)	RCC %	RMC %	RTC %
0.3wt% FeSi alloy	1.42	4.21	7.00	6.20	18.39	30.57
0.2wt% Fe-powder +0.3wt% FeSi alloy	1.53	4.78	8.00	6.68	20.81	34.93
0.4wt% Fe-powder +0.3wt% FeSi alloy	1.71	5.86	9.83	7.46	25.20	42.93

Wedge = W3; Width B=22.9mm; CM=0.35cm

Meanwhile, the difference between the single treated iron and the double treated irons varies in respect of the cooling modulus (i.e. between the wedge samples) and the inoculation treatments effect. For W_1 wedge sample, the difference between the single treated iron and the double treated irons decreases as reported in a similar study [18] whereas, in W_2 wedge sample, the difference varies as it increases at 0.4wt% Fe-powder + 0.3wt% FeSi but decreases at 0.2wt% Fe-powder+ 0.3wt% FeSi while in W_3 wedge sample the difference increases at both double treated irons (0.2wt% Fe-powder+ 0.3wt% FeSi and 0.4wt% Fe-powder+ 0.3wt% FeSi) [18]. These differences at both double treated irons led to a high chill tendency especially with RCC (16.92%) for 0.2wt% Fe-powder+ 0.3wt% FeSi and 19.34% for 0.4wt% Fe-powder+ 0.3wt% FeSi. This was due to fast solidification rate at highest cooling rate (W_1) and the effect of iron powder as it leads to high chill tendency [19,20].

In figure 5, the single treated iron for W_1 wedge sample (highest cooling rate) resulted into a relative clear chill RCC comparable to double treated W_3 wedge (medium cooling rate) solidified iron, while the mottled and total chill evaluation of single treated iron for W_1 wedge sample is also comparable to double treated W_3 wedge iron fig. 6 and 7 [18]. However, the difference in comparison between W_1-W_2 of double treated iron increases in relation with chill evaluation criteria (i.e. RTC is larger than RMC and RCC) but W_2-W_3 decreases as RCC is larger than as RMC and RTC at 0.2wt% Fe-powder while at 0.4wt% Fe-powder the comparison difference between W_1-W_2 and W_2-W_3 decreases (i.e. RCC is larger than as RMC and RTC) in both cases of comparisons.
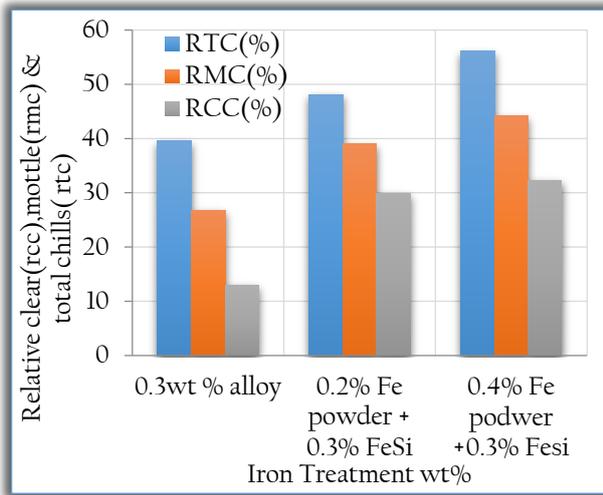
Figure 2: Effect of Inoculation Treatment on RCC, RMC, RTC for W_1
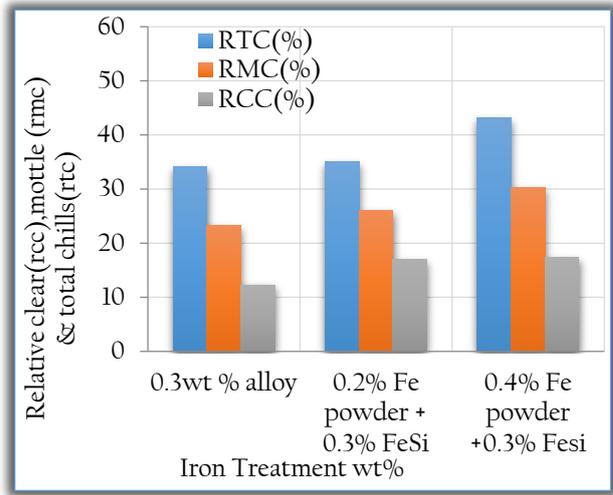
Figure 3: Effect of Inoculation Treatment on RCC, RMC, RTC for W_2
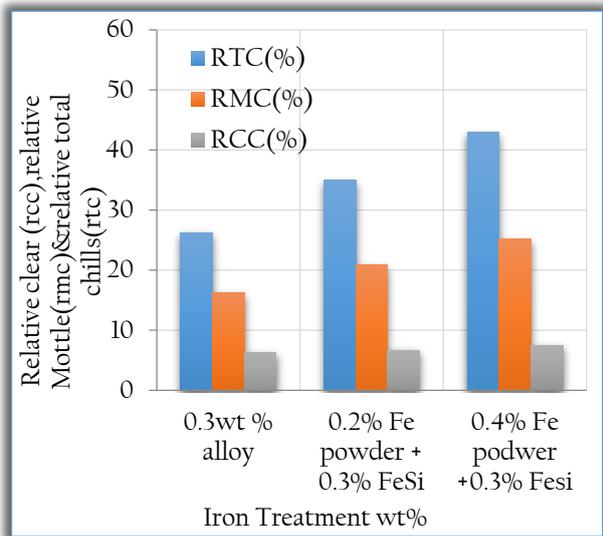
Figure 4: Effect of Inoculation Treatment on RCC, RMC, RTC for W_3
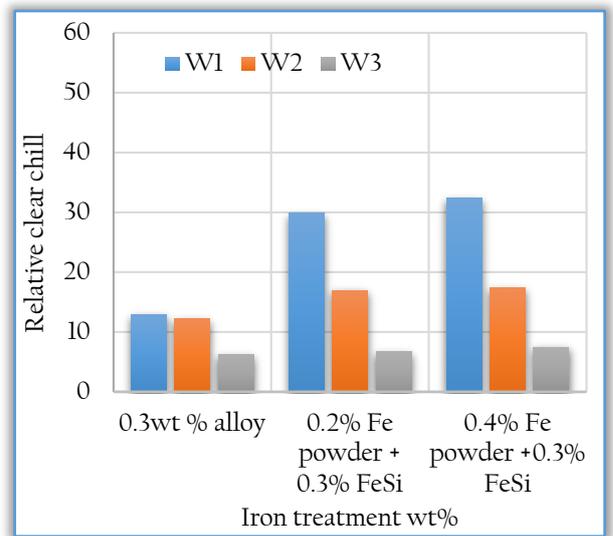
Figure 5: Comparison Difference of RCC Between W_1, W_2 and W_3
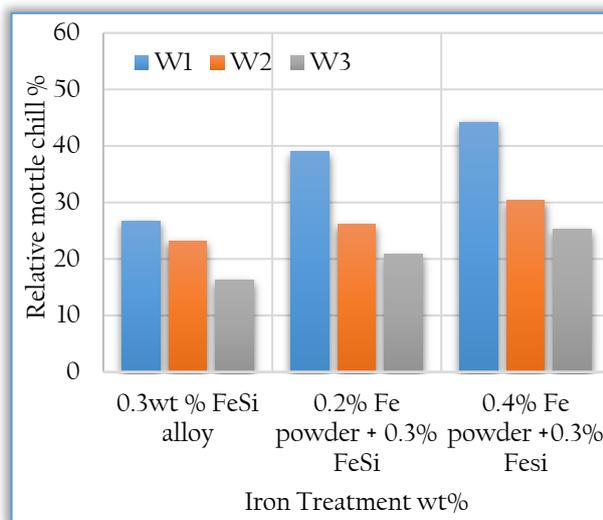

Figure 6: Comparison Difference of RMC Between W_1, W_2 and W_3
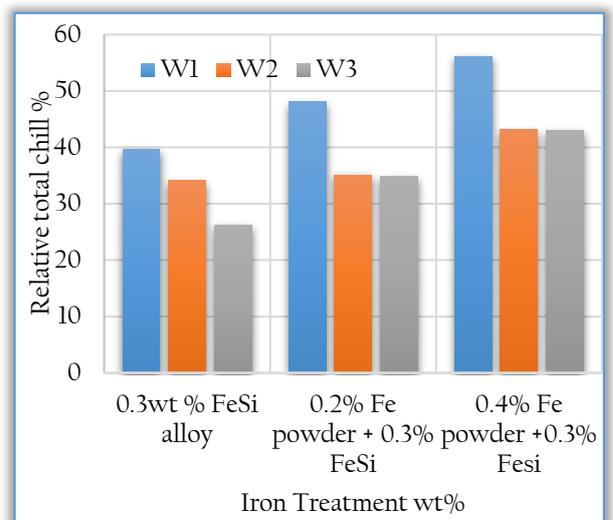
Figure 7: Comparison Difference of RTC Between W_1, W_2 and W_3

- **Microstructure analysis**

The micrograph of wedge test sample W_1 as presented in Table 5 shows that the chill zone consists of very fine, thin and close network of interdendritic graphite flakes accompanied in between by graphite inclusions.

The micrograph of the mottled zone revealed that the formation of TYPE-A graphite flakes has begun with more dispersed graphite inclusions observed while the grey zone reveals further growth of very fine TYPE-A graphite flakes randomly oriented and uniformly distributed with few areas of TYPE-D interdendritic graphite. The presence of these inclusions were due to fast rate of solidification (rapid cooling rate), improper inoculants addition and somehow fading of inoculation treatment which cause the incomplete graphitization at eutectic solidification and euctectoid transformation despite the fact that the chemistry of the single treated iron indicates high carbon and silicon content (Table 1) and also possesses aluminium content which is within the recommended range (0.005-0.01%). Also, the ratio of silicon to carbon (Si/C ratio) of the treated iron as shown in Table 6 was 0.8 which correspond to the range (0.7-0.9) at which interdendritic graphite forms up at higher solidification rates [18,21]. More so, the MnS compounds possess less ability to nucleate graphite leading to Type-D graphite at higher cooling rate [13, 22].

Table 5: Graphite Morphology/Distribution of Single Treated Iron (0.3wt% FeSi Alloy addition) for W_1, W_2 and W_3 at X200

Iron Treatment	Wedge Sample	Grey Zone	Mottle Zone	Chill Zone
0.3wt% FeSi	W_1			
	W_2			
	W_3			
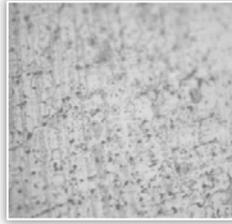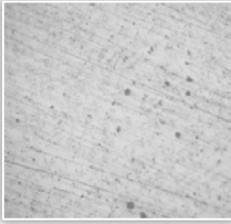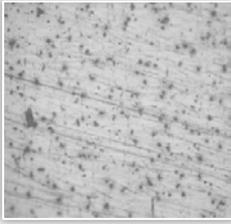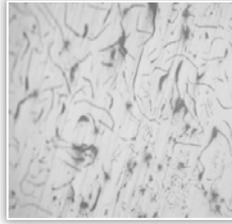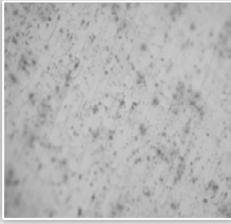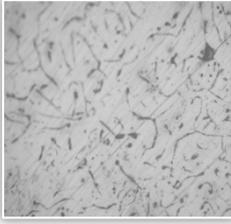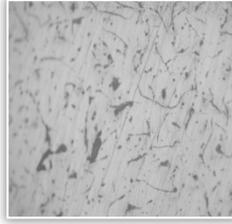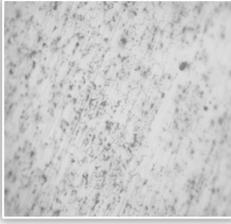
Referring to Table 5, the micrograph of the chill zone of wedge test sample W_2 is similar to that of W_1 described above but not closely spaced. As the cooling increases to the mottled zone, the microstructure revealed a distinct change in the graphite morphology, as primary TYPE-A graphite was observed with a trace of TYPE-B rosette graphite which form as a result of low degree of nucleation due to poor inoculation. This effects the eutectic solidification to begin at a larger undercooling. While the grey zone revealed very uneven distribution and randomly oriented Type –A graphite flakes which are very fine, short and thin with much graphite inclusions (point graphite). This imperfect type-A was as a result of bad solidification behaviour at the base point, metallography process (during grinding) as the flakes could be broken down due to contact with abrasives which are harder and polished microstructure exhibit globular/semi-globular regions indicating dropped ones [23].

Also shown in Table 5, the microstructure of wedge test sample W_3 where the chill zone revealed that there is a finer structure of TYPE-D interdendritic graphite flakes with very small areas of finer structure of Type - A graphite flakes. The small area of Type-A was due to the effect of inoculation despite the poor treatment and some other factors such as the high %Mn×%S (0.086) [18] which was above the recommended range (0.03-0.06) [4]. The mottled zone resulted to a morphology consisting of fine, thin and fairly uniform distribution and random orientation of Type-A graphite flakes. However, there is a little change in the morphology as the cooling proceeded to the grey zone which consists of more perfectly random oriented and uniformly distributed Type-A graphite.

The form and amount of this Type-A might be as a result of the incomplete secondary graphitization due to the improper MnS compound which serves as a major nucleation sites for graphite (particularly at second

stage of graphitization) [18,24]. Also, the high superheating which might hinders direct graphite formation by dissolving graphite promoting solid inclusion [1].

Table 6: Effect of C-Si and Si-C Ratios on the Microstructure of Irons Produced.

Iron Treatment	Carbon (C)	Silicon (Si)	C/Si Ratio	Si/C Ratio	CE
Treated (0.3wt% FeSi Alloy)	3.61	2.91	1.24	0.8	4.60
0.2wt%Fe-Powder+0.3wt% FeSi Alloy	3.99	2.49	1.60	0.6	4.86
0.4wt%Fe-Powder+0.3 wt% FeSi Alloy	4.04	2.45	1.65	0.6	4.89

In Table 7, the micrographs showed the microstructure morphology of 0.2wt% Fe- Powder + 0.3%wt FeSi alloy for wedge test sample W1 at various points. The chill zone consist of very five Type-D interdendritic graphite because the fine flakes formed at larger degree of undercooling due to fast cooling and at this point the iron powder has less ability to nucleate graphite thereby leading to Type-D graphite due to the negative effect of Fe-Powder on MnS compound characteristics, despite the FeSi inoculants treatment after iron powder addition, high carbon equivalent (CE = 4.86), %Mn X %S (0.06) was found to be in the last section of recommended range [18]. But the low level of residual aluminium (0.0013%) which is below the recommended range (0.005-0.010%) led to Type-D graphite as it affects the eutectic undercooling and recalescence degree [18, 25]. Meanwhile, the mottle zone consisted of fine and thinner structure of Type-A graphite uniformly distributed and randomly oriented with slag inclusions in between the flakes. The moderate cooling rate at this point shows that there was a decreased undercooling due to the addition of the inoculants (FeSi alloy). The high carbon and silicon content (CE = 4.86) also favoured the increase in graphitization potential which happen to be effective as a function of section sensitivity [18, 26]. However, the high carbon and silicon content, proper %Mn*%S (MnS=0.051) which was within the range (0.03-0.06), proper inoculation treatments influence the formation of Type-A graphite despite low level of aluminium content. But the grey zone revealed imperfect or uneven distribution of Type-A graphite with random orientation. Though the flakes are thicker still maintain the size compared to the middle point. This confirms the secondary graphitization occurrence.

The micrographs of W2 wedge test sample in Table 7 for 0.2wt% iron powder (Fe- Powder) + 0.3%wt FeSi alloy revealed that the chill zone has a very finer structure of Type-A graphite which is fairly distributed and randomly oriented with few areas of Type-B. Also, the mottle zone consists of fine structure of Type-A graphite with random orientation and uneven distribution. While the grey zone showed fine structure of Type-A graphite with uniform distribution and random orientation. However, the analyses of the above microstructures confirm that chill zone was able to experience incomplete secondary graphitization due to rapid cooling and section thickness. Despite this, the undercooled graphite was able to be prevented mainly because of the FeSi alloy treatment after iron powder addition and also chemistry of the melt. Meanwhile, the mottled zone micrograph was due to the moderate cooling rate which resulted into partially completed secondary graphitization with the influence of the alloy treatment and little or no effect of the iron powder while the grey zone confirmed that the thicker section undergoes a slower rate of cooling which resulted into complete graphitization.

Also in Table 7, the micrographs of W3 wedge test sample depicted the microstructure morphology of treated (0.2wt% iron powder (Fe- Powder) + 0.3%wt FeSi alloy) iron with the chill zone showing very finer structure of Type-A graphite flakes uniformly distributed and randomly oriented alongside few areas of Type- D and some point graphite's. This signifies the combine effect of the double treatment (Fe-Powder + FeSi Alloy) as the casting section thickness increases despite fast cooling rate. Whereas, the mottled zone consists of fairly uniform distributed and randomly oriented, thick and fine Type-A graphite flakes. While microstructure of the grey zone observed on the micrograph shows a complete uniformly distributed and randomly oriented finer flakes of Type-A graphite. This is as a result of high degree of nucleation, and disengaging of eutectic structure completely [1] which is more pronounce at slow rate of solidification.

Table 8 refers to the micrographs of 0.4wt% Fe- Powder + 0.3%wt FeSi alloy treatment for W_1, W_2, and W_3 wedge test samples at three points respectively. The chill zone of W_1 showed very finer structure of Type-B rosette graphite and small areas of finer structure of Type-D interrdendritic graphite with graphite inclusions in between which might be due to high superheating, slow pouring rate, etc. The micrograph of the mottled zone (W_1) showed randomly oriented but uneven distribution of very finer Type-A graphite. The Type-B disappeared as a result of increase in carbon content [1], which in turn increases the graphitization potential [18, 26]. As a result of this more graphite formation is observed [20]. Likewise, the grey zone revealed Type-A graphite (uniformly distributed and randomly oriented). Occasionally, very small area of Type-C (kish graphite) was observed (a hypereutectic graphite form) due to high carbon equivalent (CE = 4.89) but the point was able to form Type-A graphite due to effect of FeSi alloy treatment after iron powder addition. Despites slow pouring rate, extremely low aluminium content (< 0.0010) and proper %Mn*S% (0.05%).

Table 7: Graphite Morphology/Distribution of Double Treated Iron (0.2wt% Fe-Powder + 0.3wt% FeSi Alloy addition) for W_1, W_2 and W_3 at X200

Iron Treatment	Wedge Sample	Grey Zone	Mottle Zone	Chill Zone
0.2wt% Fe-Powder + 0.3wt% FeSi	W_1			
	W_2			
	W_3			
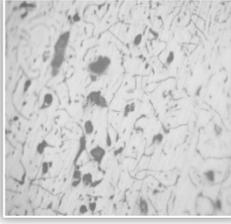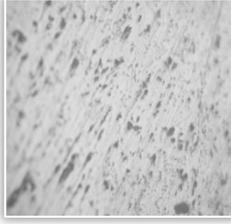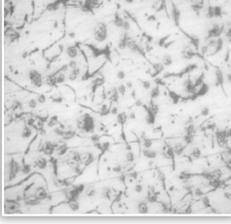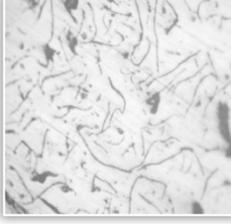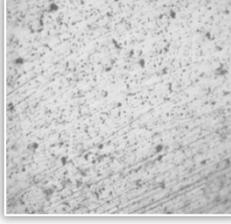
Table 8: Graphite Morphology/Distribution of Double Treated Iron (0.4wt% Fe-Powder + 0.3wt% FeSi Alloy addition) for W_1, W_2 and W_3 at X200

Iron Treatment	Wedge sample	Grey Zone	Mottle Zone	Chill Zone
0.4wt% Fe-Powder + 0.3wt% FeSi	W_1			
	W_2			
	W_3			
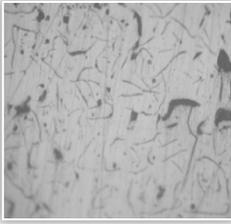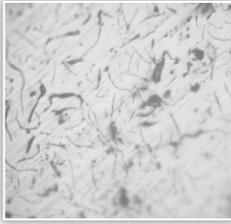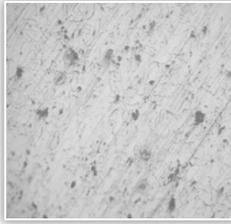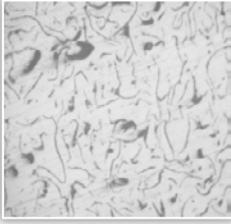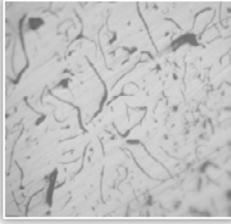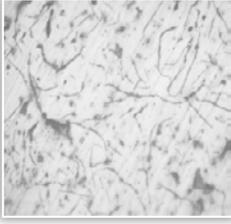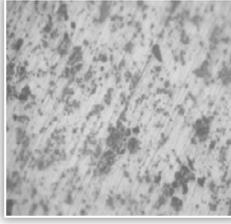
Table 8 also shows the micrographs of W_2 (0.4wt% Fe-Powder + 0.3wt% FeSi alloy). The microstructure the chill zone consists of Type-D interdendritic graphite which is due to the high rate of cooling resulting into large undercooling. The mottled zone micrograph revealed that there is primarily fine and thick Type-A graphite and small area of Type-B rosette graphite. Aside the cooling rate and section thickness, other factors

remain the same as stated above for W_1 wedge sample. While the grey zone revealed uniformly distributed and randomly oriented finer Type-A graphite.

The resulted microstructure was due to the cooling rate, in relation to the section thickness (thicker section on the wedge sample). Despite other factors such as high superheating, slower pouring rate or holding time and the effect of iron powder addition at 0.4wt% with 0.3wt% FeSi alloy treatment.

Similarly, Table 8 shows that the chill zone for W_3 wedge sample was very fine Type-D graphite with inclusions in between whereas, the mottled zone revealed very few coarse flakes (Type-A) with uniform distribution and random orientation. This would have been as a result of formation of large austenite dendrites due to the effect of iron powder on primary austenite dendrites during eutectic liquid solidification and section thickness (related to cooling rate). While the grey zone showed more refined Type-A graphite flakes not coarse as those observed in the middle point, having random orientation and fairly uniform distribution. It was observed that on slow cooling rate, the graphite morphology tends to be a little more refined at the grey zone (a dependency on section thickness). Also, high carbon and silicon content influenced more graphite formation at this point.

Table 9: Graphite Flakes Type and Size Range of the Irons

Iron Treatment	Wedge sample	Graphite Type			Graphite Size Range		
		Tip	Mid	Base	Tip	Mid	Base
0.3wt% FeSi Alloy	W_1	D	A(D)	A(D)	8	5-6	6
	W_2	D	A(B)	A	7	4	6
	W_3	D(A)	A	A	7	5	4-5
0.2wt% Fe-Powder + 0.3 wt% FeSi Alloy	W_1	D	A	A	8	5	5
	W_2	A	A	A	6	5	5
	W_3	A	A	A	7	4	5
0.4wt% Fe-Powder + 0.3 wt% FeSi Alloy	W_1	B(D)	A(D)	A(C)	6	4-5	4
	W_2	D	A(B)	A	8	4	5
	W_3	D	A	A	7	4	3-4

As shown in Table 9, it was observed that the chill zones for W_1, W_2 and W_3 revealed Type-B or Type-D, and this could be due to the effect of iron powder addition at 0.4wt% especially in thin sections as it has a limited graphitizing effect experienced at high cooling rates [27] despite the 0.3wt% FeSi treatment after the iron powder addition.

Generally, it was observed that from single treated iron (FeSi alloy treatment) to various double treated irons, the graphite amount increases as the cooling modulus increases and also graphite morphology tend to be more promoted and refined from large undercooling (undercooled graphite) to moderate undercooling (medium-sized Type-A graphite) more especially at the grey and mottled zones of single treated (0.3wt.% FeSi alloy) and 0.2wt.% Fe-powder + 0.3wt.% FeSi alloy respectively.

4. CONCLUSIONS

— It was also shown that from single treated iron (FeSi alloy treatment) to various double treated irons (iron powder addition + FeSi alloy treatment) the graphite amount increases as the cooling modulus increases and also graphite morphology tend to be more promoted and refined from large undercooling (undercooled graphites) to moderate undercooling (medium-sized Type-A graphite) more especially at the base and middle points of single treated(0.3wt.% FeSi alloy) and 0.2wt.% Fe-powder + 0.3wt.% FeSi alloy.

— The grey cast iron produced revealed varying size of graphite flakes which are randomly oriented and more pronounced at moderate and slow cooling rates.

— Despite poor inoculation, the Ca-Zr-Al-FeSi alloy inoculation treatment still has a greater effect in reducing chill in thin section castings.

— The double treated irons (0.2wt% Fe powder + 0.3wt% FeSi alloy and 0.4wt% Fe powder + 0.3wt% FeSi alloy) proved to have given the optimum iron powder addition.

— The double treatments resulted into intermediate chill and medium-sized Type A graphite with more desirable performance obtained by inoculation treatment (0.3wt% FeSi) after iron powder addition at 0.2wt%. The double treatments of iron powder addition followed by inoculation can be recommended at least for strongly hypereutectic grey cast irons. The beneficial effect of iron powder addition as secondary treatment was able to control the chill tendency favourably especially at 0.2wt% Fe-powder.

References
[1]   Singh, V.: Physical Metallurgy. Standard Publishers Distribution, 1705 Nai Sarak, New Delhi-110006. Pp. 446-463, 2009.
[2]   Strobi S: Fundamentals of green sand preparation and control, modern casting, 2000
[3]   Elkem Foundry Products: Cast Iron Inoculation- The Technology of Graphite Shape Control Booklet. www.foundry.elkem.com, 2007.

[4] Gundlack, R: Observations of Structure Control to Improve the Properties of Cast Irons. The 2008 Honorary Cast Iron Lecture, Div. 5, AFS Metalcasting Congress, Atlanta, Paper 08-158, 2008.

[5] Fraś, E., Górny, M., Kapturkiewicz, W. and López, H: Chilling Tendency and Chill of Cast Iron, Tsinghua Science and Technology ISSN 1007-0214 11/20 Vol. 13, No 2, pp.177-183, 2008.

[6] Stan, S., Chisamera, M. and Riposan, I: Solidification pattern of hypoeutectic grey cast iron in wedge test samples, POLITEHNICA University of Bucharest, Romania, Metallurgical International, Vol. XIV, special issue No. 2, pp 27-29, 2008.

[7] Elmquist L, Diószegi A and Svidró P: Key Engineering Materials 457, pp. 61 – 66, 2008.

[8] Elmquist, L., Adolfsson, S. and Diószegi, A: Characterizing shrinkage porosity in grey cast iron using microstructure investigation', AFS Trans. 116, pp. 691 – 703, 2008.

[9] Ruff, G. F. and Wallace, J. F: effect of solidification structures on the tensile properties of grey iron, AFS Trans., 85 Pp. 179 -202, 1977.

[10] Glover, D., Bates, C. E. and Monroe, R: The relationships among carbon equivalent, micro-structure and solidification characteristics and their effects on strength and chill in grey cast iron. AFS Trans. 90: pp. 745-757, 1982.

[11] Diószegi, A., Liu, K. Z., Svensson, I. L: Inoculation of Primary Austenite in Grey Cast Iron International Journal Cast Metals Research.20 (2), Pp. 68 –72, 2007.

[12] Elmquist, L. and Diószegi, A.: Int. J. Cast Metals. Res. 23, pp. 240 – 245, 2010.

[13] American Society for Testing of Material, ASTM Standard A367-60: Standard Test Methods of Chill Testing of Cast Iron. West Conshohocken: ASTM; page 2, 2005.

[14] Seidu S.O. and Ogunniyi I. O. (2012): Control of Chilling Tendency in Grey Cast Iron Reuse. Material Research vol.16 no.1 São Carlos Jan./Feb. 2013 Epub Nov 22, 2012 ISSN 1516-1439

[15] Seidu S.O.: Inoculants effect on chilling tendency in Ductile Iron. In: Proceedings of the International PhD Foundry Conference; 2009; Brno. Brno University of Tchnology; 2009.

[16] Riposan I, Chisamera M, Stan S and White D.: Chilling properties of Ba/Ca/Sr inoculated grey cast irons. International Journal of Cast Metals Research, 20(2), pp. 90-97, 2007.

[17] Riposan, I., Chisamera, M., Stan, S., Toboc P., Ecob C., white D: Al,Zr-FeSi Preconditioning of Grey Cast Iron", Material Science and Technology, Vol. 24 (5), pp 578-584, 2008.

[18] Saka S. O., Seidu S. O., Taiwo A. S and Riposan I.: Chilling Effect of Iron Powder on the Microstructure and Hardness Property of Strongly Hypereutectic Grey Cast Iron. Annals Faculty of Enginering, Hunedoara, Int. J. Engineering, Vol. 17 Issue 4, Pp 13 – 22, 2019.

[19] Chisamera M., Riposan I., Stan S., and Barstow M.: Structure Characteristics of Iron Powder Treated Slightly Hypereutectic Grey Irons, Int. J. Cast. Metals. Res., 2011, 24(6), pp 370–377, 2011.

[20] Riposan, I., Chisamera, M., Stan, S. and Barstow, M.: Influence of Iron Powder Addition on the Solidification and Structure of Slightly Hypereutectic Grey Cast Iron, AFS Trans., 119, p 389–406, 2008.

[21] Bockus, S.: A Study of the Microstructure and Mechanical Properties of Continuously Cast Iron Products. METABK 45 (4) pp. 287-290, 2006.

[22] Elkem AS Foundry Products Division: Cast Iron Inoculation- The Technology of Graphite Shape Control, ISO 9001, 2012.

[23] Riposan, I., Chisamera, M., Stan, S. and Barstow, M.: Improving Chill Control in Iron Powder Treated Slightly Hypereutectic Grey Cast Iron, China Foundry, Vol. 8, No. 2, pp. 228-229, 2012.

[24] Taşliçukur, Z., Altuğ, G., Polat, Ş., Hakan, Ş., Atapek, and Türedi, E.: Characterization of Microstructure and Fracture Behavior of GG20 and GG25 Cast Iron Materials used in Valves Brno, Czech Republic, EU., 2012.

[25] Riposan, I., Chisamera, M., Stan, S., Hartung, C. and White, D.: Three-Stage Model for the Nucleation of Graphite in Grey Cast Iron, Material Science Technology 26(12), pp. 1439–1447, 2010.

[26] Chisamera, M., Riposan, I., Stan, I. and Skaland, T.: Investigation of Effect of Residual Aluminium on Solidification Characteristics of Un-Inoculated and Ca/Sr Inoculated Grey Irons. AFS Transactions, vol.107, Paper 04-096, 2004.

[27] Stefanescu, D. M.: Classification and Basic Metallurgy of Cast Iron, Metals Handbook, Vol. 1, 10th Ed. ASM International, Materials Park Ohio, USA, Pp.4-7, 1989.